A CW-PION FOCUSING HORN FOR LOW-ENERGY MUON NEUTRINO BEAMS*

T. Dombeck
Los Alamos National Laboratory, Los Alamos, NM 87545, USA

D. D. Koetke, D. S. Koetke, and R. Fisk
Valparaiso University, Valparaiso, IN 46383, USA

Abstract

Low-energy muon neutrino beams can be produced from pion decays in-flight at high-intensity accelerators, such as the Los Alamos Meson Physics Facility (LAMPF), providing a new tool to study the role of the weak interaction in nuclear and particle physics. Employing a pion focusing device can enhance the neutrino flux by large factors, and reduce backgrounds by sign-selection of the parent pions. However, LAMPF's long beam pulse and high repetition rate makes it impractical to use pulsed horns like those found at high-energy accelerators. In this paper we discuss a CW-pion focusing device that uses coils wound inside vanes mounted radially around the beam axis to provide an azimuthal field. From our studies with a prototype magnet, we have found that the optimum field configuration needed to focus pions at LAMPF energies can be obtained by adjusting the radial density of turns in the coils. This optimum yields an six-fold increase in neutrino flux above the muon threshold over the bare-target case. Our calculations also indicate a correlation between the arrival time of the neutrinos in the detector and their energy.

Neutrino Beamline and Criteria for Pion Focusing

Many important physics questions can be addressed with muon neutrino-nucleus interactions near the muon threshold [1-4]. We have finished one such experiment at LAMPF using neutrinos generated from a bare target. However, our studies indicate that a pion focusing device would have substantially increased the neutrino flux and reduced backgrounds, providing a significant improvement over our published results [2].

Fig. 1 shows schematically the in-flight pion decay neutrino beamline we used in our recent experiments at LAMPF. Proton currents up to 24 μA at 800 MeV were transported onto a bare water target [5] to generate pions. The target was 2.5 cm in diameter and 1 m in length. Those pions escaping the target were allowed to decay along a channel 12 m in length by 4 m in diameter. An 8-m thick mass of iron and magnetite shielded the detector from all particles except the neutrinos. The detector was a 2 m high cylinder of liquid scintillator, about 2 m in diameter, having a mass of 4.5 tons. It was placed behind the iron shield in a concrete block house, with its central plane 21 m from the target. The beamline and detector were placed below ground level to provide shielding on all sides.

With the bare-target arrangement we calculated fluxes in the detector to be 2.1×10^{-9} ν/cm^2-p for neutrinos above the muon threshold [6]. This yielded cross sections for breakup reactions resulting from muon-neutrino interactions with carbon nuclei in the detector that were consistent with theoretical predictions [7].

The relative location for a future pion focusing device is just downstream of the target in Fig. 1. Beside the high repetition rate that requires a CW-magnet, there are a number of additional criteria that influence the design of the LAMPF focusing device. These include: (a) since pions are generated over a large angular and kinetic energy range, dictating that the device must have a large acceptance, (b) at low pion energies absorption is large, indicating that the pions should not have to pass through any material such as

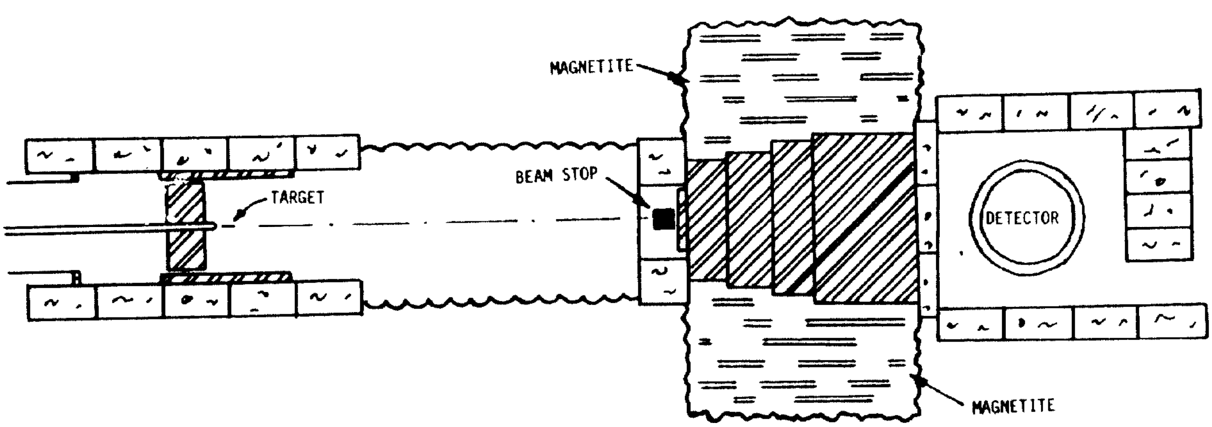

Fig. 1. The in-flight pion decay neutrino beamline at LAMPF is shown schematically. Pions generated by the interaction of the 800-MeV proton beam in the water target decayed along a 12-m long decay channel. An 8-m thick iron shield stopped all particles but neutrinos from hitting the detector placed 21 m from the target. Also shown is the relative location of a future pion focusing device.

skins on a focusing horn, (c) many low-energy pions will decay close to the target, therefore the focusing device will have to turn the pions in a short distance to be effective, and (d) high radiation levels are anticipated in the vicinity of the focusing device, dictating that mineral-insulated electrical cables are necessary.

In order to calculate the performance of a focusing device, we have used pion yield measurements for both carbon and water targets. The distribution of positive pion energies can go up to 600 MeV and change shape with production angle and incident proton energy. These distributions have been parametrized by Gaussian widths and average pion kinetic energies, for all angles and incident proton energies involved [1,5]. In order to determine the design limitations placed on the magnetic field shape of the focusing device, we calculated the magnetic rigidity ($\int B \cdot dl$) required to turn the distribution of pions generated at each angle parallel to the beam axis. This was our condition for ideal focusing. The results are plotted in Fig. 2. The error bars indicate the rms spread due to the pion kinetic energy distribution at each angle. As can be seen, for a given pion flight path through the device, the magnetic field must increase with radius, in an approximately linear fashion, to obtain the best focus.

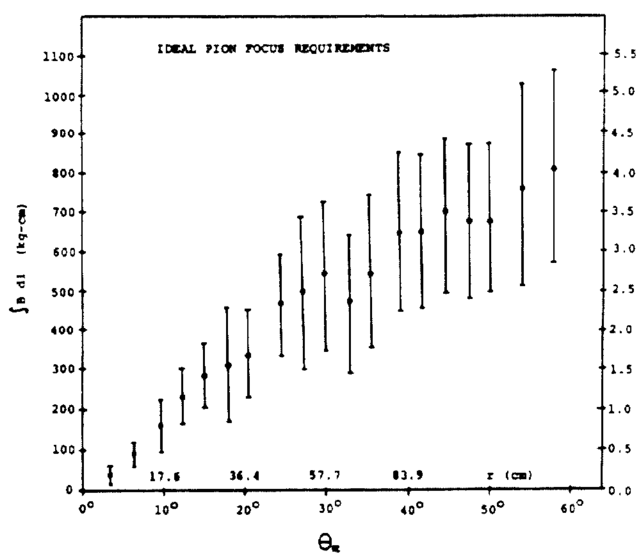

Fig. 2. Using the pion yield data summarized in ref. [1], we performed a calculation of the magnetic rigidity ($\int B \cdot dl$) necessary to turn the pions generated at a specific production angle in the target parallel to the beam axis, our condition for ideal focusing. The error bars indicate the rms spread due to the pion kinetic energy distribution at each angle. Note that the ideal focus condition indicates that a magnetic field varying linearly with radius is needed to obtain the best focus condition.

Pion Focusing Magnet Design

CW-focusing devices based on a butterfly dipole [1] and solenoidal [8] magnetic field have been proposed. However, the dipole has a reduced solid angle, and the solenoid provides no sign-selection of the pions. Our pion focusing magnet is a modified toroid, with the current loops collected into six or more long vanes around the beam axis, emanating radially outward, with free spaces between them to increase the solid angle for the pions to travel freely. This magnet produces an azimuthal field that provides focusing for one sign of pions and de-focusing for the other.

The azimuthal magnetic field produced by an N-turn wire loop carrying a current I, is given by $\mu_o NI/(2\pi r)$. Therefore, to achieve the desired field shape that varies linearly with radius, the density of wire turns must increase as r^2 outwards along the vanes. Placing such a device with six or more vanes just downstream of the target, the pions will see azimuthal magnetic field lines like that shown by the example in Fig. 3. These field lines were calculated for a six-vaned magnet using the program POISSON [9].

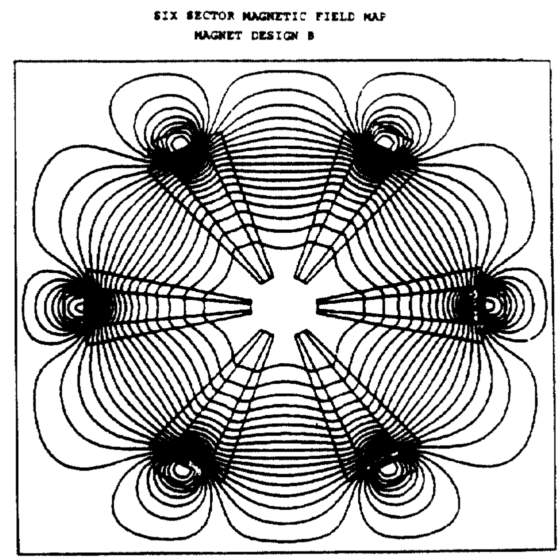

Fig. 3. A plot of the azimuthal magnetic field lines are shown for a six-vane magnet. This field was generated using the program POISSON [9]. It shows the field seen by a pion heading into the magnet. Note that there is evidence for radial components to the field that turn the pions away from the vanes as they are focused toward the beam axis. This reduces absorption losses due to pions striking the vanes, but increases absorption for the wrong-sign pions.

Pions striking the vanes will be absorbed, so there will be a loss due to the solid angle presented to the target by the upstream end of the vanes. We estimate this loss can be kept below 20%. A larger solid angle is subtended over the longitudinal length of the vanes, and more pions striking the inside surfaces of the vanes would be expected to be absorbed. However, the radial component to the magnetic field evident in Fig. 3 turns pions away from the vanes simultaneously as they are focused toward the beam axis and reduces this loss. On the other hand, the wrong-sign pions are turned toward the vanes which helps to reduce their numbers.

Field Measurements Made on a Prototype Magnet

In order to facilitate a calculation of the effect of the focusing device and the resulting neutrino flux, we constructed a prototype magnet 60-cm long, having eight vanes mounted in an aluminum cylinder with a 61-cm diameter. The wires were wrapped inside each vane with a density that increased as r^2 as required for the correct field shape. The return windings were distributed along the outside edge of the cylinder. The magnet length was not important, as we were interested in the fringe field near the magnet ends. This gave us a three-dimensional field map to be used in our Monte Carlo calculation of the flux, which otherwise would have been difficult to calculate. At the center of the magnet, where the fringe field effects were small, the resulting field shape agreed with that predicted by POISSON to within 2%.

Calculated Neutrino Flux and Optimization of Magnet Parameters

In our Monte Carlo flux calculation [6] we specified the geometry in Fig. 1 with the dimensions discussed above. We used a 30-cm long carbon target, though we believe that a 30-cm long water target will give similar results [5]. Our magnet design used in the calculation had eight vanes, each subtending about 8^o in azimuth, and having a three-dimensional field map scaled from our prototype measurements. For a magnet 120 cm in diameter, having a length of 225 cm, we found that only 19% of the positive pions struck the vanes. This confirmed our idea that pions in the magnet would be turned away from the vanes leaving only the solid angle subtended by the upstream edge of the vanes (18%) as the major loss due to pion absorption. A larger number of pions (37%) hit the outside cylinder of the magnet, but upon removing the cylinder from the calculation, we found these pions were of little use as they generally hit the channel wall before decaying. Furthermore, we found that many of the negative pions which were turned away from the beam axis by the magnet would hit the metal cylinder and be absorbed.

In the calculation we found that the optimum magnetic field had a maximum value of 3.5 kG at a radius of 60 cm. There was evidence of over-focusing if the field were raised to 4.0 kG. This optimum field strength was a weak function of the length of the magnet, which we set to 225 cm. This yielded an increase of a factor of six over the bare-target case for the neutrino flux above the muon threshold in the detector 21 meters away. In general we found that the energy spectrum also peaked about 25% higher in energy (125 MeV) for the focused spectrum, which is shown in Fig. 4 compared to the bare-target case. This increase in flux can be compared to that expected for the ideal focus case which yields a factor of 16; or a factor of 13 if we exclude the pions that are absorbed by the vanes. Thus our calculation is about a factor of two below ideal focusing. Finally, the anti-neutrino contamination from the wrong-sign pion decays is reduced to 1% from the 10% level for a bare target.

Assuming mineral-insulated hollow bore copper conductors (0.64-cm square with a 0.32-cm hole for cooling water), the power consumption for the magnet can be estimated. Our design requires a total of 110 turns per vane with a density increasing as r^2, from which we estimate the total resistance of the magnet to be 0.67 ohms. For the magnetic field strength required, we calculate a power consumption near 2.5 MW for this magnet.

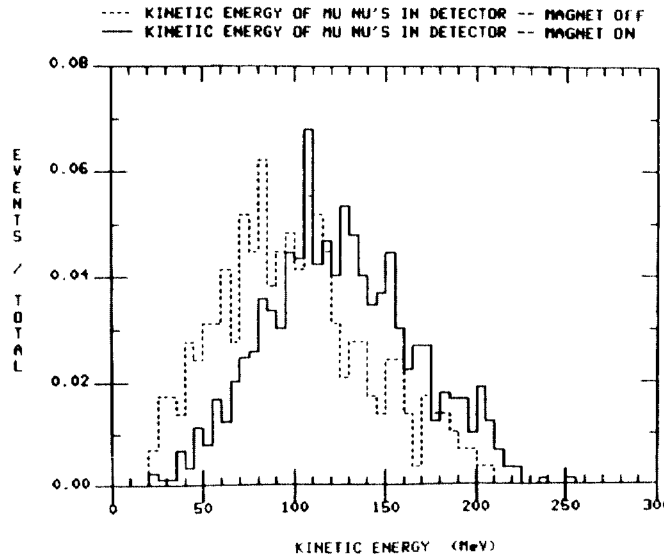

Fig. 4. The calculated neutrino energy spectrum is shown for the focusing device compared to that for a bare-target. The two histograms have been normalized to equal areas. The focusing device produces a flux that is about 25% higher in energy on average.

References

*Work performed under the Auspices of the U. S. Department of Energy.

[1] Los Alamos National Laboratory Proposal to the U.S.D.O.E. for "A High Intensity Los Alamos Neutrino Source," (1982).

[2] T. Dombeck et al., PL B194, 591 (1987).

[3] R. Burman et al., Letter of Intent to the LAMPF PAC, "The Measurement of Muon Neutrino-Electron Scattering and The Search for Neutrino Oscillations at Small Mixing Angles," (December 7, 1983).

[4] T. W. Donnelly, Prog. in Part. and Nucl. Phys. 13, 183 (1985). Also, G. VanDalen et al., "Observation of Anomalous ν_μ $^{12}C \rightarrow \mu^-$ ^{12}N Exclusive Interactions Near Threshold," (submitted to PRL).

[5] T. Dombeck et al., "Details of a Water Target Used in a High Current Application for a Neutrino Physics Experiment and the Direct Measurement of the Incident Proton Beam by the Induced Change in the Water Conductivity," (Los Alamos National Laboratory report LA-UR-88-801, submitted to NIM). Also, T. Dombeck et al., in the IEEE Proc. of the Particle Accelerator Conf., Vols I-III, 87-CH-2387-9, p. 588, (1987).

[6] T. Dombeck, "LANLNU--A Description of the Monte Carlo Computer Calculation of the Neutrino Flux at the High Intensity Los Alamos Neutrino Source," (Los Alamos National Laboratory report LA-UR-1589, 1982).

[7] R. Manweiler et al., talk presented at the Third Conf. on the Intersections between Particle and Nuclear Physics, Rockport, Maine, May 14-19, 1988.